

---

## Law of Approach to Saturation for Determining Magnetic Intrinsic Behavior of $\text{BaFe}_{12-x}\text{Mn}_{x/2}\text{Ti}_{x/2}\text{O}_{19}$ and $\text{SrFe}_{12-x}\text{Mn}_{x/2}\text{Ti}_{x/2}\text{O}_{19}$

Rafael F. Maniur<sup>1</sup>, Adam Badra Cahaya<sup>1,†</sup>, Azwar Manaf<sup>1</sup>

<sup>1</sup>Department of Physics, Faculty of Mathematics and Natural Sciences, Universitas Indonesia  
Depok 16424, Indonesia

<sup>†</sup>[adam@sci.ui.ac.id](mailto:adam@sci.ui.ac.id)

---

Submitted : August 2021; Revised : December 2021; Approved : December 2021; Available  
Online : December 2021

---

**Abstrak.** Magnet permanen medan anisotropik yang sangat tinggi adalah sulitnya untuk menentukan sifat magnetik intrinsik jika diukur menggunakan magnetometer yang memiliki medan magnet terbatas. Model matematika Law of Approach to Saturation (LAS) menyediakan cara untuk mengukur magnet permanen, dengan medan anisotropik tinggi dengan mengoreksi data magnetisasi kurva kuadran pertama atau kurva perawan dari loop histeresis minor. Dalam penelitian ini, program komputasi LAS dilakukan untuk menghitung sifat magnetik intrinsik bahan magnetik, seperti magnetisasi saturasi, medan anisotropi dan konstanta anisotropi magnetokristalin. Data magnetisasi diperoleh dari pengukuran permagraf barium heksaferit ( $\text{BaFe}_{12}\text{O}_{19}$ ), strontium heksaferit ( $\text{SrFe}_{12}\text{O}_{19}$ ) dan penyerap gelombang mikro  $\text{BaFe}_{12-x}\text{Mn}_{x/2}\text{Ti}_{x/2}\text{O}_{19}$  dan  $\text{SrFe}_{12-x}\text{Mn}_{x/2}\text{Ti}_{x/2}\text{O}_{19}$ . Pengaruh substitusi bahan barium heksaferit dan strontium heksaferit terhadap nilai magnetisasi saturasi, konstanta anisotropi dan medan anisotropik dapat dinilai dengan mengamati konvergensi nilai magnetisasi.

**Kata Kunci:** *barium heksaferit; kurva histeresis; Law of Approach to Saturation; sifat magnetik intrinsik; strontium heksaferit*

**Abstract** Permanent magnetic materials of very high anisotropic fields is that it is still difficult to determine the intrinsic magnetic properties, when measured using a magnetometer which has a limited magnetic field. The Law of Approach to Saturation (LAS) mathematical model provides a way to measure permanent magnets, with high anisotropic fields by correcting the magnetization data of the first quadrant curve or the virgin curve of the minor hysteresis loop. In this research, a computational LAS program was conducted to compute the intrinsic magnetic properties of magnetic materials, such as saturation magnetization, anisotropy field and magnetocrystalline anisotropy constant. Magnetization data of barium hexaferrite ( $\text{BaFe}_{12}\text{O}_{19}$ ), strontium hexaferrite ( $\text{SrFe}_{12}\text{O}_{19}$ ),  $\text{BaFe}_{12-x}\text{Mn}_{x/2}\text{Ti}_{x/2}\text{O}_{19}$  and  $\text{SrFe}_{12-x}\text{Mn}_{x/2}\text{Ti}_{x/2}\text{O}_{19}$  are analyzed. The convergences of magnetization were assessed to determine the effect of substitution on barium hexaferrite and strontium hexaferrite materials on saturation magnetization values, anisotropy constants and anisotropic fields. We determine the appropriate lower limit for LAS method to give correct values of saturation magnetization values, anisotropy constants and anisotropic fields.

**Keywords:** *barium hexaferrite; hysteresis loop; intrinsic magnetic properties; Law of Approach to Saturation; strontium hexaferrite.*

DOI : 10.15408/fiziya.v4i1.22206

## INTRODUCTION

To achieve a high energy density, a permanent magnet must have high remanence and coercivity values. The magnetic phase must have a high anisotropic field value so that the coercivity value is high. Both remanent and coercivity are derived from the main hysteresis loop or major hysteresis loop. Thus, to magnetize permanent magnets that have high coercivity, a high external magnetic field is required. As an illustration, the magnetic anisotropic field of Nd-Fe-B is 5.4 MA/m or 67.5 kOe [1], [2]. Therefore, a magnetizing field of 67.5 kOe is required to obtain the main hysteresis loop. This can only be achieved when using magnet magnets from superconductors[3]. However, at this time magnetization generally uses an electromagnet which can only produce a magnetic field external magnet of 12 kOe to 15 kOe [4]. Therefore, another method is needed to obtain the main hysteresis loop from the use of such a low external magnetic field.

The anisotropic field itself depends on the distance and direction of the lattice of a material to the magnetic field [5]–[7] and affects the shape of the hysteresis loop of a material. The high anisotropic field in some types of materials causes the need for new equipment to study these materials, while the magnetometer equipment can only measure in fields around 1.2 T to 1.5 T [8]. When used, the material in the magnet will produce a hysteresis loop. minor, which unfortunately does not describe the true state of the magnetic material under study. The minor loop is not a true loop, while to obtain magnetic properties, a major hysteresis loop is needed, which is difficult to obtain when measured only with a weak field magnetometer.

The use of the LAS (Law Approach of Saturation) method [9]–[11] is intended to overcome the difficulties of studying materials with very high anisotropic fields. In this method, it is hoped that materials with minor loops can be converted into major hysteresis loops, so that their magnetic properties can be explained. In addition, the LAS method can determine the intrinsic properties of a material, namely anisotropic fields, anisotropic constants, and saturation [10], which are useful for the purposes of making magnetic materials or for modifying these magnetic materials.

## LAW OF APPROACH TO SATURATION METHOD

For this study, we were looking for material data sets of Mn-Ti-substituted barium hexaferrite ( $\text{BaFe}_{12-x}\text{Mn}_{x/2}\text{Ti}_{x/2}\text{O}_{19}$ ) and strontium hexaferrite ( $\text{SrFe}_{12-x}\text{Mn}_{x/2}\text{Ti}_{x/2}\text{O}_{19}$ ). Material data sets were using Permagraph from Ref. [4]. These material data sets were used to validate the executed program as well as for hysteresis loop correction purposes, with the magnetization data taken is the minor hysteresis loop of magnetization data in the first quadrant *i.e.* from the beginning of the magnetization until the magnetization value reaches the peak. Figure 1 shows the hysteresis loop and the virgin curve of the selected data of Barium Hexaferrite and Strontium Hexaferrite, to be used for validation.

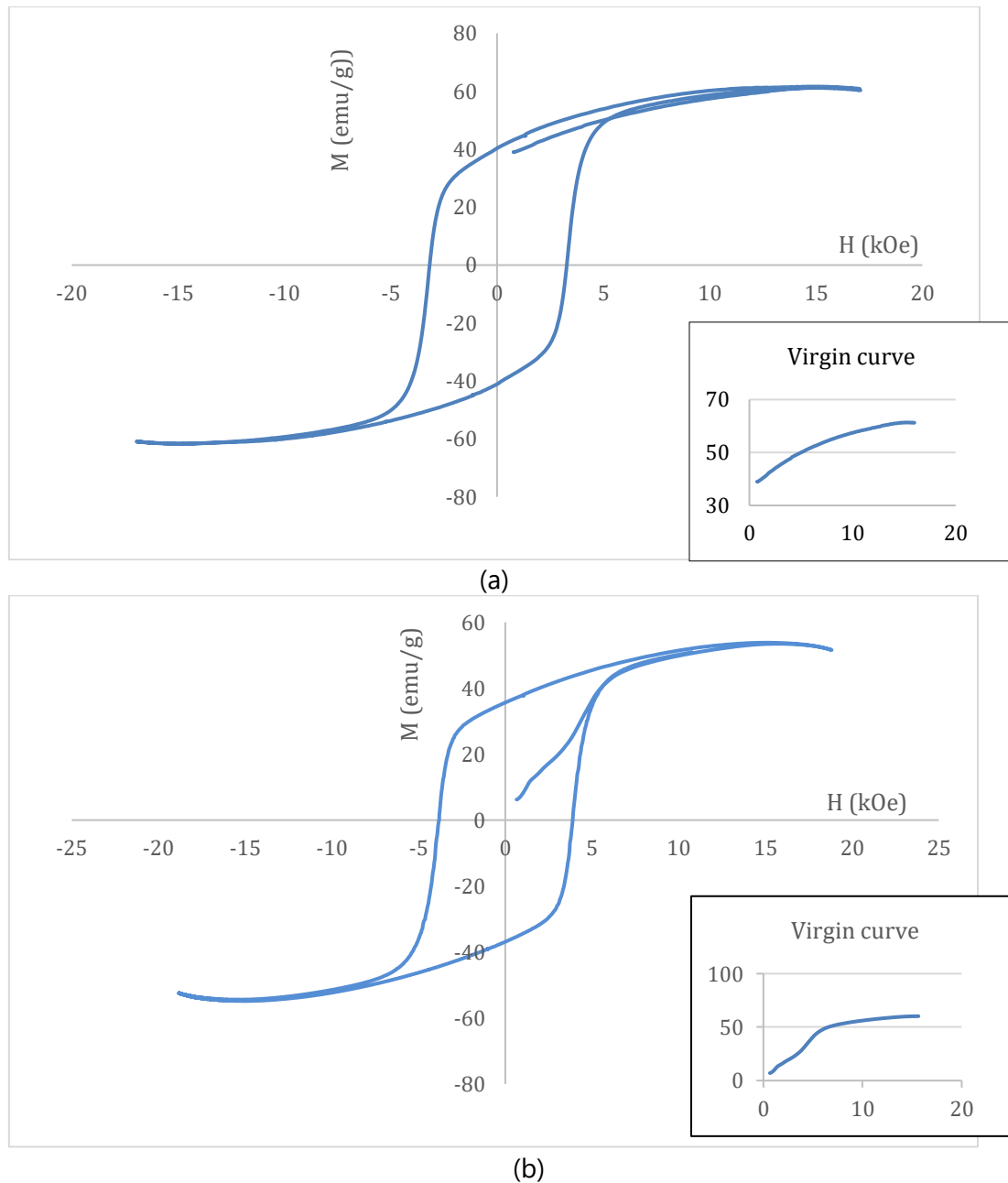


**Figure 1.** Hysteresis Loop and virgin curve (inset) of (a) barium hexaferrite (BaFe<sub>12</sub>O<sub>19</sub>) and (b) strontium hexaferrite (SrFe<sub>12</sub>O<sub>19</sub>)

As can be seen from Figure 1 saturation in magnetization occurs when the magnetization of a material stops or rises very slowly when a very large external magnetic field is applied. This behaviour of magnetization curve is often called Law of Approach to Saturation (LAS)[12]. While there are variations in the approximation for LAS, in this study we compare 4 models: Akulov [10], Brown [11], Grössinger [12] and Néel [13]. The most general the most general of them is Grössinger equation.

$$M = M_s \left[ 1 - \frac{a}{H} - \frac{b}{H^2} - \frac{c}{H^3} \right] + \chi H \quad (1)$$

This equation is a generalized equation from Akulov approximation ( $a = c = \chi = 0$ ) [10], Néel approximation ( $c = \chi = 0$ ) [13] and Brown approximation ( $c = 0$ ) [11]. Here  $M_s$  is magnetization saturation,  $\chi$  is magnetic susceptibility,  $a > 0$  is inhomogeneity parameter,

$b$  and  $c$  are related to magnetic anisotropy [12]. While in Ref. [12] another  $\sqrt{H}$  term that arises from spin wave is considered, we ignore this term for better comparison with other LAS models. The value of  $b$  is related to anisotropy constant  $K_1$  (or anisotropy field  $H_a = 2K_1/M_s$ ) as follows [6], [12].

$$b = \frac{8}{105} \times \frac{K_1^2}{M_s^2} = \frac{2}{105} H_a^2 \quad (2)$$

Eq. (2) shows that with a positive  $b$  value, the intrinsic magnetic properties of a material, such as anisotropy constant and anisotropic field can be determined. A positive value for the constant  $b$  also indicates that the field is sufficient to produce the calculated  $M_s$  value of a material, while a negative value indicates that the applied magnetic field is not sufficient to make a material achieve saturation magnetization.

## RESULTS AND DISCUSSION

To determine a suitable model to find the saturation magnetization value in a material, we fit the data in Figure 1(a) with LAS models in Eq. (2). As shown in Figure 2, the application of the Brown model and the Grössinger model produces a magnetization value that continues to increase when an external magnetic field  $H$  is up to 40 kOe. These models are not in line with the principle of saturation of the magnetization. Néel and Akulov models, however, shows signs of reaching the saturation magnetization value at a certain external field value. The plot of the magnetization value calculated by the two models shows a difference in the value. The results obtained that the saturation magnetization values in the Néel and Akulov models are 62 emu/gr and 58 emu/gr, respectively.

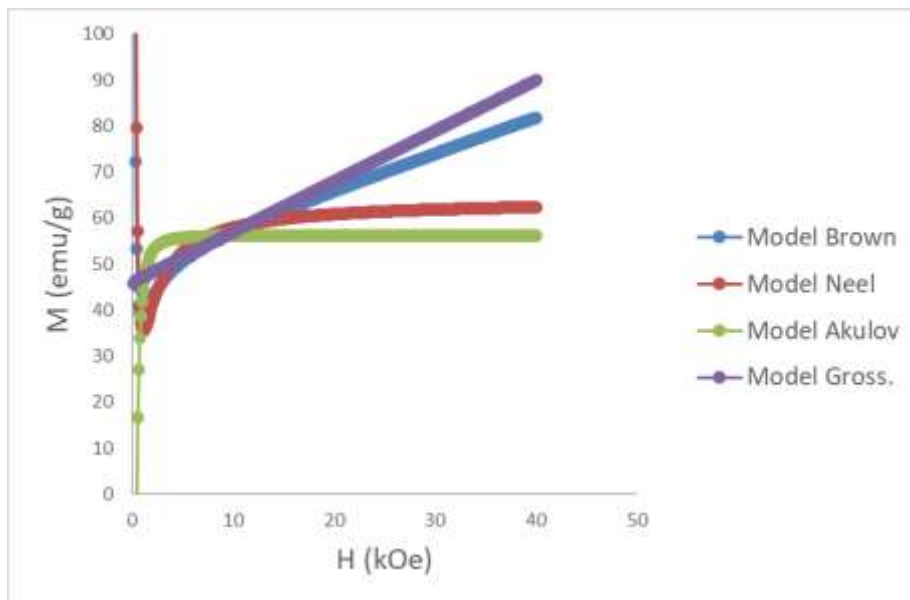


**Figure 2.** M vs H of Law of Approach to Saturation (LAS) models of materials BaFe<sub>12</sub>O<sub>19</sub>.

The  $M_s$  value of the computational result is compared with the  $M_s$  value of barium hexaferrite material from the literature, which is  $M_s = 72$  emu/g or 0.48 T [14]. We can conclude that  $M_s$  value in the Néel model is closer to the literature value compared to

the saturation magnetization value in the Akulov models. Therefore, we will use Néel model for further fitting.

$$M = M_s \left[ 1 - \frac{a}{H} - \frac{b}{H^2} \right] \quad (3)$$

To ensure  $M_s$  convergence, we determined a suitable lower limit to determine the value of  $M_s$ . We suggest that a good lower limit for fittings occurs by plotting the magnetization saturation value when fitting at some variation of the lower limit value against a given external field, with error bars presented to help seeing the convergence of the magnetization values on a visible graph.

### Lower Limit Fitting for Realistic $a$ and $b$

A good lower limit is determined when the  $M_s$  error value generated when fitting with a lower limit variation is small, and there is convergence (no change) in the  $M_s$  value after setting the lower limit variation. These conditions are then applied to determine the saturation magnetization value and a good field lower limit value for this material. A plot of  $M_s$  vs lower limit  $H$  with variation of 1 kOe to 10 kOe of  $\text{BaFe}_{12}\text{O}_{19}$  composition is shown on figure 3. When the  $H$  field around 8500 Oe the  $M_s$  value begins to decrease from the  $M_s$  value of about 68 emu/g, which is close to the reference value  $M_s$  of  $\text{BaFe}_{12}\text{O}_{19}$  (72 emu/gr). This saturation magnetization value also improves the saturation magnetization value obtained before the lower limit is applied. This shows that a good lower limit will produce a good saturation magnetization value as well.

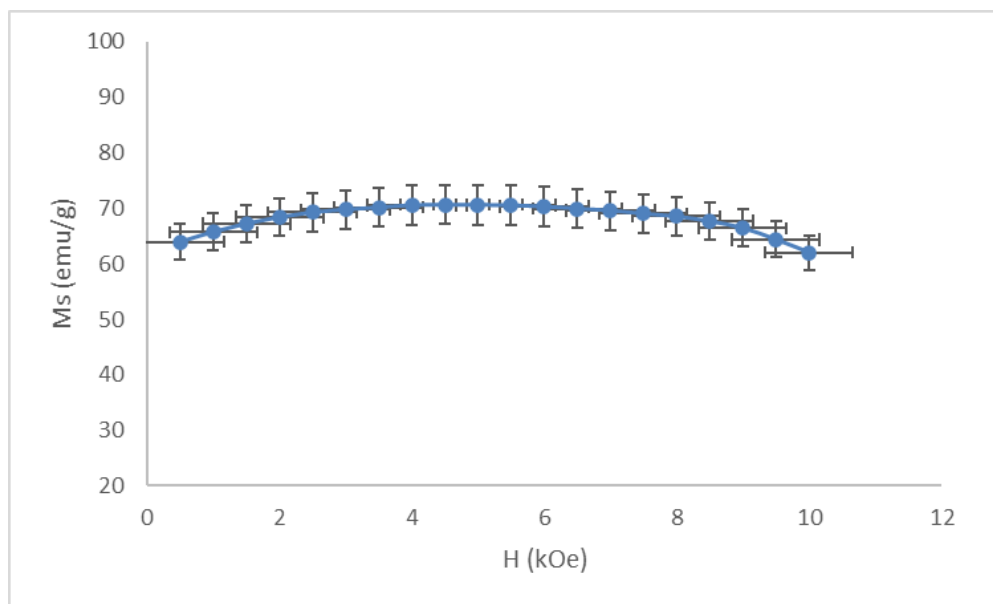


**Figure 3.** LAS method requires appropriate choice for its lower limit  $H$ . Here the fitting result for  $M_s$  is plotted against the lower limit  $H$  that is varied between 1 kOe to 10 kOe on the composition of  $\text{BaFe}_{12}\text{O}_{19}$ .

Next,  $a$  and  $b$  are observed to determine the right lower limit as it is very influential on the calculation results of the intrinsic magnetic properties of a material. The value of  $a$  and  $b$  are illustrated in Figure 5. Since  $a > 0$  and  $b = 2H_a^2/105$ , the determination of

the lower limit value requires that the values of  $a$  and  $b$  are positive quantities. Figure 4 indicates that  $a$  and  $b$  are positive for 8.5 to 9.5 kOe.

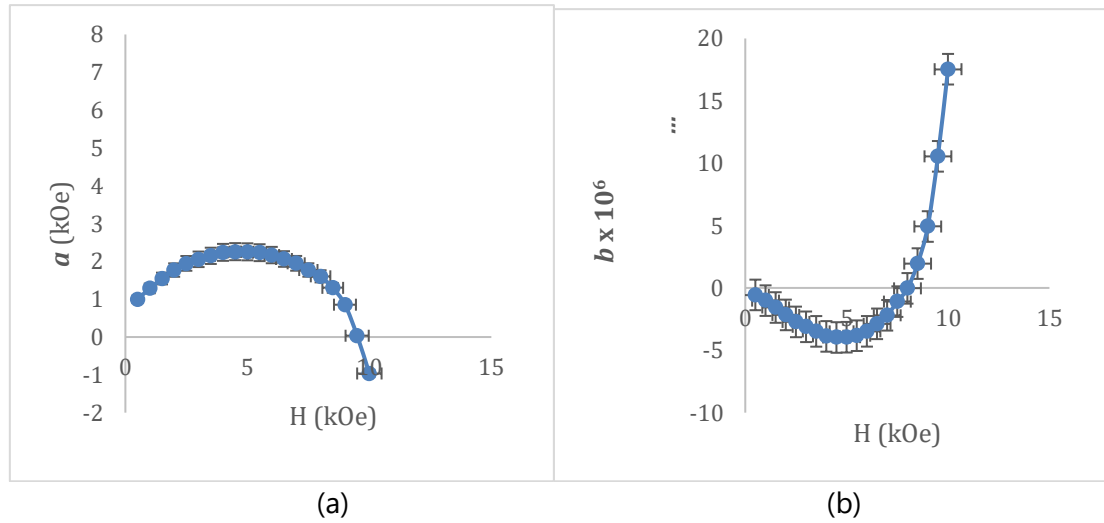


**Figure 4.** Compared to  $M_s$ , values of (a)  $a$  constant and (b)  $b$  constant are plot against the lower limit  $H$  for LAS method of  $BaFe_{12}O_{19}$  material.

Table 1 summarized the calculation results of the LAS method for pure BHF samples. We calculated the intrinsic magnetic properties of pure BHF materials and compared them with reference values. The calculated data is also used to determine a suitable lower bound. These intrinsic magnetic properties include the value of saturation magnetization, the value of the anisotropy constant ( $K_1$ ) and the anisotropy field ( $H_a$ ). The lower limit between 8.5 kOe to 9.5 kOe was then chosen to find the value of the anisotropy constant  $K_1$  and the anisotropic field  $H_a$  at each lower limit.

**Table 1.** The intrinsic magnetic properties resulting from the variation of the lower limit between 8.5 kOe, 9 kOe, and 9.5 kOe in  $BaFe_{12}O_{19}$  materials compared with literature values [14]

Lower Limit (kOe)	$M_s$ (emu/g)		$K_1$ ( $10^6$ erg/cc)		$H_a$ (kOe)	
	Fit.	Lit.	Fit.	Lit.	Fit.	Lit.
8.500	68	72	3.42	3.3	10.123	16.994
9.000	66	72	5.34	3.3	16.079	16.994
9.500	64	72	7.57	3.3	23.535	16.994

By choosing 8.5 kOe as lower limit for LAS analysis, the anisotropic constant and the anisotropic field yield values of  $3.42 \times 10^6$  erg/cc and 10.123 kOe, respectively, approaching the theoretical value of  $3.3 \times 10^6$  erg/cc and 16,994 kOe [17]. In Figure (43), the lower limit values of the 2.0 kOe and 8.5 kOe external fields produce the same saturation magnetization value, but because the lower limit of 2.0 kOe produces a negative  $b$  constant value, this situation can be ignored. This shows that the lower limit of the external magnetic field of 8.50 kOe is a good lower limit for determining the intrinsic magnetic properties of pure  $BaFe_{12}O_{19}$  materials.

## Saturation Magnetization and Anisotropy field of $\text{BaFe}_{12-x}\text{Mn}_{x/2}\text{Ti}_{x/2}\text{O}_{19}$ , and $\text{SrFe}_{12-x}\text{Mn}_{x/2}\text{Ti}_{x/2}\text{O}_{19}$

After validating the calculated data from the LAS method of  $\text{BaFe}_{12}\text{O}_{19}$  magnetization data, this computational program can be applied to calculate the intrinsic parameters of the synthesized material. In this section, the results of the calculation of the LAS method on data from two different Radar Absorbing Material (RAM) samples are discussed, namely  $\text{BaFe}_{12-x}\text{Mn}_{x/2}\text{Ti}_{x/2}\text{O}_{19}$ , and  $\text{SrFe}_{12-x}\text{Mn}_{x/2}\text{Ti}_{x/2}\text{O}_{19}$ , which were calculated using the Néel model with limits under an external field of 500 kA/m respectively. with  $x = 0.1$  sample of both RAM is given. We note here that values of  $a$  for  $\text{SrFe}_{12-x}\text{Mn}_{x/2}\text{Ti}_{x/2}\text{O}_{19}$  are small enough, such that Néel model does not differ much from Akulov model for  $\text{SrFe}_{12-x}\text{Mn}_{x/2}\text{Ti}_{x/2}\text{O}_{19}$ .

Table 2 and 3 are the summary of intrinsic magnetic values of both RAM materials of  $\text{BaFe}_{12-x}\text{Mn}_{x/2}\text{Ti}_{x/2}\text{O}_{19}$ , and  $\text{SrFe}_{12-x}\text{Mn}_{x/2}\text{Ti}_{x/2}\text{O}_{19}$ , respectively The substitution of  $\text{Mn}^{2+}$  and  $\text{Ti}^{4+}$  ions to  $\text{Fe}^{3+}$  ions change the intrinsic magnitude of the material phase [18]. There is a downward trend in the values of  $M_s$ ,  $H_a$ ,  $K_1$ , and  $b$  when Mn-Ti substitution is given ( $x > 0$ ). It may be because the substitution of Mn-Ti ions in both RAM material influences the dimensions of the  $\text{BaFe}_{12}\text{O}_{19}$  crystal unit cell due to the difference in the size of the radii of Mn and Ti ions with Fe ions [17].

The virgin curve magnetization data were obtained with a very limited external magnetic field of 12 – 15 kOe or 960 - 1200 kA/m. The fitting result have been summarized for the respective RAM samples in Tables 2 and 3. The intrinsic value of the magnetic properties of the magnetic phase of the material is expected to be used by other researchers to conduct data analysis and further discussion of the experimental test results.

**Table 2.** Output of computational results of the LAS sample  $\text{BaFe}_{12-x}\text{Mn}_{x/2}\text{Ti}_{x/2}\text{O}_{19}$  ( $x=0; 0.1; 0.3$  and  $0.5$ )

Comp. X	$M_s$ (T)	$H_a$ (kA/m)	$K_1 \times 10^5$ (J/m <sup>3</sup> )	B (kA/m) <sup>2</sup>
0	0,418	1613	3,37	49583
0,1	0,433	1698	3,67	54932
0,3	0,411	1444	2,97	39767
0,5	0,391	1268	2,48	30631

**Table 3.** Output of computational results of the LAS sample  $\text{SrFe}_{12-x}\text{Mn}_{x/2}\text{Ti}_{x/2}\text{O}_{19}$  ( $x=0; 0.1; 0.3; 0.5;$  and  $1.0$ )

Comp. X	$M_s$ (T)	$H_a$ (kA/m)	$K_1 \times 10^5$ (J/m <sup>3</sup> )	b (kA/m) <sup>2</sup>
0	0,36	1739	3,13	57460
0,1	0,321	1659	2,66	52485
0,3	0,338	1445	2,44	39776
0,5	0,344	1577	2,71	47375
1,0	0,36	1498	2,7	42769

## CONCLUSION

From this study, we can conclude that the Law of Approach to Saturation (LAS) method using magnetization data from the minor loop works based on an appropriate mathematical model. The Néel model can be applied for both namely  $\text{BaFe}_{12-x}\text{Mn}_{x/2}\text{Ti}_{x/2}\text{O}_{19}$ , and  $\text{SrFe}_{12-x}\text{Mn}_{x/2}\text{Ti}_{x/2}\text{O}_{19}$ . Lower limit selection for this study plays a significant part since it greatly determines the convergence of saturation magnetization. Furthermore, lower limit selection is required to determine correct values for  $a$  and  $b$ . Positive values of  $a$  and  $b$  can be obtained by selecting 8.5 kOe lower limit for LAS method.

## ACKNOWLEDGMENTS

The authors would thank L. Darmawan for experimental discussion.

## REFERENCES

- [1] J. J. Croat, J. F. Herbst, R. W. Lee, and F. E. Pinkerton, "High-energy product Nd-Fe-B permanent magnets," *Applied Physics Letters*, vol. 44, no. 1, pp. 148–149, Jan. 1984, doi: 10.1063/1.94584.
- [2] J. Mohapatra and J. P. Liu, "Chapter 1 - Rare-Earth-Free Permanent Magnets: The Past and Future," vol. 27, E. B. T.-H. of M. M. Brück, Ed. Elsevier, 2018, pp. 1–57. doi: <https://doi.org/10.1016/bs.hmm.2018.08.001>.
- [3] J. van Nugteren, "High Temperature Superconductor Accelerator Magnets," 2016.
- [4] L. Darmawan, Suparno, and A. Manaf, "Enhancement of Magnetic and Microwave Absorbing Properties of  $[\text{Ba}(\text{Fe}, \text{Mn}, \text{Ti})_{12}\text{O}_{19}]_{1-x}-[\text{CoFe}_{12}\text{O}_4]_x$  ( $x = 0.2; 0.5; 0.8$ ) Composites," *Journal of Physics: Conference Series*, vol. 1485, p. 12046, 2020, doi: 10.1088/1742-6596/1485/1/012046.
- [5] A. Renuka Balakrishna and R. D. James, "A tool to predict coercivity in magnetic materials," *Acta Materialia*, vol. 208, p. 116697, 2021, doi: <https://doi.org/10.1016/j.actamat.2021.116697>.
- [6] F. Kools and A. Morel, "Ferrite Magnets: Improved Performance," K. H. J. Buschow, R. W. Cahn, M. C. Flemings, B. Ilshner, E. J. Kramer, S. Mahajan, and P. B. T.-E. of M. S. and T. Veyssi re, Eds. Oxford: Elsevier, 2004, pp. 1–5. doi: <https://doi.org/10.1016/B0-08-043152-6/01908-2>.
- [7] P. Gruszecki, C. Banerjee, M. Mruczkiewicz, O. Hellwig, A. Barman, and M. Krawczyk, "Chapter Two - The influence of the internal domain wall structure on spin wave band structure in periodic magnetic stripe domain patterns," in *Recent Advances in Topological Ferroics and their Dynamics*, vol. 70, R. L. Stamps and H. B. T.-S. S. P. Schulthei , Eds. Academic Press, 2019, pp. 79–132. doi: <https://doi.org/10.1016/bs.ssp.2019.09.003>.
- [8] R. Prigl, U. Haeberlen, K. Jungmann, G. zu Putlitz, and P. von Walter, "A high precision magnetometer based on pulsed NMR," *Nuclear Instruments and Methods in Physics Research Section A: Accelerators, Spectrometers, Detectors and Associated Equipment*, vol. 374, no. 1, pp. 118–126, 1996, doi: [https://doi.org/10.1016/0168-9002\(96\)37493-7](https://doi.org/10.1016/0168-9002(96)37493-7).
- [9] E. C. Devi and I. Soibam, "Effect of Zn doping on the structural, electrical and magnetic properties of  $\text{MnFe}_2\text{O}_4$  nanoparticles," *Indian Journal of Physics*, vol. 91, no. 8, pp. 861–867, 2017, doi: 10.1007/s12648-017-0981-7.
- [10] H. Zhang, D. Zeng, and Z. Liu, "The law of approach to saturation in ferromagnets originating from the magnetocrystalline anisotropy," *Journal of Magnetism and Magnetic*



- Materials*, vol. 322, no. 16, pp. 2375–2380, 2010, doi:  
<https://doi.org/10.1016/j.jmmm.2010.02.040>.
- [11] B. D. Cullity and C. D. Graham, *Introduction to Magnetic Materials*. John Wiley & Sons, 2011.
- [12] R. Grössinger, "A critical examination of the law of approach to saturation. I. Fit procedure," *physica status solidi (a)*, vol. 66, no. 2, pp. 665–674, Aug. 1981, doi:  
<https://doi.org/10.1002/pssa.2210660231>.
- [13] N. S. Akulov, "Über den Verlauf der Magnetisierungskurve in starken Feldern," *Zeitschrift für Physik*, vol. 69, no. 11, pp. 822–831, 1931, doi: 10.1007/BF01339465.
- [14] W. F. Brown, "Theory of the Approach to Magnetic Saturation," *Physical Review*, vol. 58, no. 8, pp. 736–743, Oct. 1940, doi: 10.1103/PhysRev.58.736.
- [15] R. Grössinger, "A critical examination of the law of approach to saturation. I. Fit procedure," *physica status solidi (a)*, vol. 66, no. 2, pp. 665–674, Aug. 1981, doi:  
<https://doi.org/10.1002/pssa.2210660231>.
- [16] L. Néel, "Relation entre la constante  $d$  d'anisotropie et la loi d'approche à la saturation des ferromagnétiques," *Journal de Physique et le Radium*, vol. 9, no. 6, pp. 193–199, 1948, doi: 10.1051/jphysrad:0194800906019300.
- [17] R. C. Pullar, "Hexagonal ferrites: A review of the synthesis, properties and applications of hexaferrite ceramics," *Progress in Materials Science*, vol. 57, no. 7, pp. 1191–1334, 2012, doi:  
<https://doi.org/10.1016/j.pmatsci.2012.04.001>.
- [18] G. Turilli, F. Licci, S. Rinaldi, and A. Deriu, "Mn<sup>2+</sup>, Ti<sup>4+</sup> substituted barium ferrite," *Journal of Magnetism and Magnetic Materials*, vol. 59, no. 1, pp. 127–131, 1986, doi:  
[https://doi.org/10.1016/0304-8853\(86\)90019-3](https://doi.org/10.1016/0304-8853(86)90019-3).
- [19] M. H. Shams, A. S. H. Rozatian, M. H. Yousefi, J. Valíček, and V. Šepelák, "Effect of Mg<sup>2+</sup> and Ti<sup>4+</sup> dopants on the structural, magnetic and high-frequency ferromagnetic properties of barium hexaferrite," *Journal of Magnetism and Magnetic Materials*, vol. 399, pp. 10–18, Feb. 2016, doi: 10.1016/J.JMMM.2015.08.099.